p-ISSN 2089 – 0133 e-ISSN 2477-6416
URL: https://jurnal.uns.ac.id/ijap/article/view/86355

DOI: https://doi.org/10.13057/ijap.v15i1.86355

# A THEORETICAL STUDY OF ELECTRON IMPACT EXCITATION OF THE LOWEST AUTOIONIZING STATES OF RUBIDIUM USING A DISTORTED WAVE METHOD

**Fredrick Omboga Oketch***
Department of Mathematics and Physics, Technical University of Mombasa, Mombasa, Kenya
*fomboga@tum.ac.ke

Received 01-05-2024, Revised 18-10-2024, Accepted 28-11-2024,
Available Online 01-04-2025, Published Regularly April 2025

## ABSTRACT

In this study, we applied distorted wave method to calculate integral cross sections, differential cross sections, and alignment parameters for electron impact excitation of the lowest autoionizing state of Rb. The projectile electron energy we considered is in the range of near threshold up to high energy region (1 keV). We considered static potential of the initial target state as the initial channel distortion potential and a linear combination of static potentials of initial and final target states as the final channel distortion potential. The wave functions used in this model are the multi-zeta and the double-zeta Hartree-Fock single electron wave functions. In order to perform the numerical calculations, we have modified distorted wave Born approximation 1 (DWBA1) program. In the present study, we have evaluated the exchange amplitudes exactly without any approximation. We have compared our results with other theoretical and experimental results available to us. The present results for integral cross sections are in good agreement with experimental results of Borovik. Our distorted wave results are in much better agreement with the experimental result than does the Dirac *B*-spline *R*-matrix results of Borovik. Additionally, our alignment parameter results show a near threshold maximum. Furthermore, from the present differential cross sections results it is observed that when the incident energy increases to 200 eV, the cross sections with or without the effect of exchange coincide nearly at all scattering angles.

Keywords: Integral cross-sections; differential cross sections; distorted wave; distortion potential; alignment parameter.

**Cite this as:** Oketch, F. O. 2025. A Theoretical Study of Electron Impact Excitation of The Lowest Autoionizing States of Rubium Using a Distorted Wave Method. IJAP: Indonesian Journal of Applied Physics, 15(1), 59-72. doi: https://doi.org/10.13057/ijap.v15i1.86355

## INTRODUCTION

Atomic collisions involve scattering induced by impact of either electrons, protons, positrons, photons, ions or neutrons by a target in the form of an atom or an ion. Major physical quantities of interest in scattering are cross sections, which can be differential or integral, alignment and angular correlation parameters [1]. Over the years, these studies have been extensively investigated through experiment [2-7] or by applying known theoretical models [6, 8-13]. Besides, the study of autoionizing states of atoms has generated a lot of interest over time because of its underlying importance in the understanding of atomic structures and the dynamics of their excitation process. In particular, the contribution of excitation of these levels by charged particles impact has been used to successfully explain the presence of resonance structures in

ionization. Some results have been reported on electron impact excitation of the lowest autoionizing states of alkalis [12-13] and the other references therein. However, the discrepancy between the experimental and theoretical results has not been fully addressed. Furthermore, only a few studies [12,14] have reported differential cross section results and angular correlation parameters despite their better reliability in testing any theoretical model as compared to integral cross sections.

The study of electron - ejected spectra after collisional excitation of ionization of alkali metals (Li, Na, K, Rb and Cs) [2-8, 11-14] is very instrumental in the investigation of autoionizing states. From the anisotropic emission of electrons relative to the incident particle beam, more explicit details of the collision process, the relative excitation or ionization cross section of magnetic substates of the autoionizing or Auger states can be studied. The collisional excitation of a state by particle impact leads, in general, to an alignment of the excited state, i.e., the magnetic substates are populated differently. Thus, the measurement of the alignment gives, besides the total cross sections, further information on the excitation process. In the case of an autoionizing state the alignment can be determined via the non-isotropic angular distribution of ejected electrons relative to the beam direction of the incident projectile particles [1,15]. In general, the anisotropy depends on the alignment and the Auger transition amplitudes and phases.

Ross and Ottley [2] observed autoionizing transitions in rubidium by measuring the energy spectrum of electrons ejected perpendicular to the direction of an incident 500 eV electron beam. In another study, Srivastava and Rai [8] applied the method suggested by Crothers and McCarroll [16] to the study of electron impact excitation of autoionizing levels in alkali metal atoms. The major assumption here is that the autoionizing levels arise from the excitation of an inner-shell electron to the valence shell. Nygaard [3] experimentally studied autoionizing levels in Cs, Rb, and K by electron impact. He compared his findings with the results of theoretical calculations of Roy and Rai [17]. An important conclusion was that the effects of autoionization and inner-shell ionization had been overestimated in the theory. Tiwary and Rai [11] used a radial wave function that had been suggested by Clementi [18] to calculate total cross-sections for the electron impact excitation of the lowest autoionizing levels in the Rb, Cs and K atoms. They applied the first-Born approximation, modified first Born approximation and Vainshtein approximations (neglecting exchange). Stapelfeldt *et al*., [4] performed an experimental study of autoionizing states of the negative rubidium ion in a strong resonant laser field and discussed the role of autoionizing states in multiphoton double-ionization processes. Furthermore, they used electron spectroscopy to show that double ionization of $Rb^-$ primarily is the result of a sequential removal of the two electrons via an excited Rb state.

Kaur and Srivastava [12] performed relativistic distorted-wave (RDW) calculations for the electron impact excitation of the lowest autoionizing states in Na, K, Rb and Cs atoms from the ground state using spin resolved Dirac-Fock wave functions. Detailed results in the range of near threshold to 1.5 keV incident electron energies were obtained for total cross sections of the magnetic sub states of the individual $^2P_{3/2}$ and $^2P_{1/2}$ states. The results obtained were not in very good agreement with other previously reported results. In another study, Pangantiwar and Srivastava [13] performed Distorted-wave calculations for electron (and positron) impact excitation of lowest-lying autoionizing levels in alkalis (Li, Na, K, Rb and Cs) for incident particle energy varying above the threshold energy of the atom to 600 eV. In their study, appropriate initial- and final-state static potentials were used for distorting the incident and scattered projectile electron (and positron) waves, respectively. They also used multi-zeta HF wave functions of Clementi and Roetti [18].

Borovik *et al*., [6] experimentally studied the near-threshold excitation dynamics of the autoionizing states in rubidium atoms by measuring the ejected-electron excitation functions and theoretically by applying a fully relativistic Dirac *B*-spline *R*-matrix (DBSR) model. They observed that strong negative-ion resonances dominate the electron-impact excitation of the lowest autoionizing states in Rb. Elsewhere, Borovik *et al*., [7] measured the total normalized intensities of ejected-electron spectra arising from the decay of the $4p^5b_1l_1n_2l_2$ autoionizing levels. They investigated the electron impact energy range from the $4p^6$ excitation threshold at 15.31 eV up to 50 eV. They found that the $4p^6$ excitation–autoionization is the dominant indirect ionization process contributing over 30 % of the total single ionization of rubidium atoms by electron impact in the 15.3 – 50 eV energy range.

Unlike lithium, sodium and potassium, rubidium has not received adequate attention. For *Li, Na* and *K*, the electron exchange plays an important role in studying the collision for resonance *S* - *P* type excitations. To describe scattering of this process fully we require the complex amplitudes for triplet and singlet modes, i.e., when the spins of target and incident electrons are parallel and antiparallel to each other respectively. One assumes that explicitly spin-dependent forces such as the spin-orbit interaction between projectile and target may be neglected. In a collision process between the polarized projectile electron with a polarized target, the triplet and singlet scattering modes will have different amplitudes. This gives rise to a difference between spin parallel and spin antiparallel scattering leading to a spin asymmetry in the polarized electron-polarized atom collision. The study of the angular variation of the spin asymmetry and spin resolved orientation parameters would provide detailed information on the scattering bringing out the role of exchange. For instance, whereas Matterstock *et al*., [22] measured alignment parameter for the lowest autoionizing state of potassium from the threshold to 1000 eV, DuBois *et al*., [23] reported strong resonances near the excitation threshold in their alignment parameter of the lowest autoionizing fine structure states of sodium. From this point of view, we find that the electron impact excitation of the lowest autoionizing states of the lighter alkalis have received extensive attention [22-26] and several theoretical and experimental results [2-8,11-14] are available for both differential cross sections and angular correlation parameters as well as spin parameters.

The present work therefore considers electron impact excitation of spin unresolved lowest autoionizing level of rubidium. We have used distorted wave method (DWD) by employing a variation suggested by Singh [10]. The range of projectile energies considered is from the excitation threshold to high energy region. In this study, we have used multi-zeta Hartree-Fock wave functions of Clementi and Roetti [18] to calculate integral cross sections, differential cross sections, and alignment parameters. Furthermore, for comparison purposes, we used the double-zeta wave functions. We have also calculated the exchange amplitude exactly without making any approximation in the distorted wave first Born approximation. For our numerical calculations, we modified the code originally developed by Madison and Bartschat [19] for electron-hydrogen scattering from an *s* state to higher orbital states. The major difference between our calculations and other distorted wave approaches [12-14] is in the choice of the arbitrary distortion potential. We have employed the initial state static potential as the initial distortion potential and a simple average of the initial state static potential and the final state static potential as the final distortion potential.

## THEORETICAL MODEL

The excitation processes that we have considered for our calculations are expressed as

$$e_i^- + Rb\left[4p^6 5s^1, {}^2S_{1/2}\right] \rightarrow e_s^- + Rb^+\left[4p^6\, {}^1S_0\right] + e_e^- \quad (1a)$$

$$e_s^- + Rb^*\left[4p^5 5s^2\, {}^2P_{1/2}, {}^2P_{3/2}\right] \quad (1b)$$

where, $e_i$, $e_5$, and $e_6$ represent incident, scattered and ejected electrons, respectively. Here, the first process (equation 1*a*) gives only the contribution from direct ionization of the Rb atom, while in the second process (equation 1*b*) ionization takes place as a two-step process, i.e., first the Rb atom is excited to either the $4p^5 5s^2$, $^2P_{1/2}$ or $4p^5 5s^2\, ^2P_{3/2}$ state, which then in a second step autoionizes by ejection of electrons leading to ionization. In this excitation process we assume that the transitions only involve one atomic electron, that is 4*p* - 5*s, in* rubidium. Thus, we have treated it as behaving like one electron system.

In the distorted wave approximation, the transition matrices for electron impact excitation of one electron atom [19] are expressed as

$$T^{dir} = \left\langle \chi_f^-(r_o)\psi_f(r_1) \middle| V(r_o, r_1) \middle| \chi_i^+(r_o)\psi_i(r_1) \right\rangle \quad (2)$$

for direct excitation, and

$$T^{ex} = \left\langle \chi_f^-(r_0)\psi_f(r_1) \middle| V(r_0, r_1) \middle| \chi_i^+(r_1)\psi_i(r_0) \right\rangle \quad (3)$$

for exchange excitation.

In Equations 2 and 3 $\Psi_{i(f)}$ represents the initial (final) state target atom wave function. We have used the multi zeta Hartree-Fock Slater type orbitals [18] to represent the single electron atomic wave functions in either initial or final state. The function $\chi^{(+)}$ represents the distorted waves with incoming (outgoing) wave boundary conditions and $U_{i(f)}$ is the distortion potential experienced by the target atom in its initial (final) state.

The distorted waves are obtained by solving the following second order differential equations:

$$(\nabla_0^2 + k_f^2 - U_f)\chi_f^- = 0 \quad (4)$$

$$(\nabla_0^2 + k_i^2 - U_i)\chi_i^+ = 0 \quad (5)$$

, where, $k_{i(f)}^2$ is the initial (final) kinetic energy of the projectile electron given in Rydberg units. In the present work the distortion potentials that we have used in Equations 4 and 5 are evaluated as

$$U_i = \left\langle \psi_i \middle| V \middle| \psi_i \right\rangle \quad (6)$$

and

$$U_f = \frac{1}{2}\langle \psi_i | V | \psi_i \rangle + \frac{1}{2}\langle \psi_f | V | \psi_f \rangle \quad (7)$$

This choice for the distortion potentials is necessitated by the reasoning that when the projectile is in the initial state, for all the time it is in the field of the initial state of the target, the distortion potential should therefore be taken as the static potential of the target atom in its initial state. When the energy from the projectile electron is transferred to the target atom, the atom takes time (relaxation time) to go to its final state. That is, there is a time lag between the time of transfer of energy and the instant when the atom reaches its final state. Thus, the projectile electron in its final state 'sees' a potential which is intermediate between the initial- and final-state static potentials. Hence the final state distortion potential has been taken as the sum of one-half of the initial state static potential and one-half of the final state static potential of the target atom [10].

In Equations 2, 3, 6 and 7 $V$ is the electron-atom interaction potential expressed as

$$V = -\frac{1}{r_0} + \sum_{i=1}^{N} \frac{1}{r_{0i}} \quad (8)$$

where $r_0$ and $r_{0i}$ are the projectile electron-target nuclear interaction term and the projectile electron–target electron interaction term, respectively.

The transition matrices in Equations 2 and 3 were evaluated first and then used in calculating integral cross sections, differential cross sections, and alignment parameters. In order to evaluate the direct and exchange scattering amplitudes given above, the radial distorted waves $\chi_f^+$ and $\chi_f^-$ were first expanded in terms of the partial waves as

$$| \chi_i^+ \rangle = \sqrt{\frac{2}{\pi}} \frac{1}{k_i r} \sum_{li,mi} i^{l_i} \chi_{l_i}(k_i, r) Y^*_{l_i mi}(k_i) \quad (9)$$

and

$$| \chi_f^- \rangle = \sqrt{\frac{2}{\pi}} \frac{1}{k_f r} \sum_{l_f, m_f} i^{l_f} \chi^*_{l_f}(k_f, r) Y_{l_f m_f}(r) Y^*_{l_f m_f}(k_f) \quad (10)$$

In Equations 9 and 10, $Y_{lm}$ is a spherical harmonic. In the expansion of $\chi_f^-$ in Equation 10, the complex conjugate of the radial part $\chi_{lf}$ is taken so that it satisfies the incoming wave boundary conditions. Substituting the above partial wave expansions of the distorted waves in the Equations 4 and 5, one gets the radial wave equations as

$$\left[ \frac{d^2}{dr^2} - \frac{l_s(l_s+1)}{r^2} - U_s(r) + k_s^2 \right] \chi_{l_s}(r) = 0 \quad (11)$$

In Equation 11, $s=i$ for initial state and $s=f$ for the final state distorted wave. In the asymptotic region they satisfy the boundary condition: $\lim_{r\to\infty} \chi_{ls}(k_s,r) = j_{ls} + B_{ls}(-\eta_{ls}+ij_{ls})$ . Here, $j_l$ and $\eta_l$ are regular and irregular Ricatti-Bessel functions, and $B_l$ is given as $B_l = exp(i\delta_l)sin\,\delta_l$, where $\delta_l$ is the elastic scattering phase shift. The radial distorted wave equation, Equation 11, for initial and final states is solved using Numerov's method. We have expanded the transition matrices fully by making use of vector addition coefficients (Clebsch-Gordon coefficients).

Moreover, the incident electron was considered to be along the z-axis for purposes of simplifying the problem [19].

The differential cross-sections, defined as the probability of scattering per unit incident flux per unit solid angle, are obtained using the relation:

$$\left(\frac{d\sigma}{d\Omega}\right)_{4p\to 5s} = \frac{1}{4\pi^2}\frac{k_f}{k_i}\sum_{m=-1}^{+1}\left[\frac{1}{4}\left|T^{dir}_{4p\to 5s} + T^{ex}_{4p\to 5s}\right|^2 + \frac{3}{4}\left|T^{dir}_{4p\to 5s} - T^{ex}_{4p\to_{5s}}\right|^2\right] \quad (12)$$

The total cross-sections are the probability of scattering per unit incident flux and are obtained by summing all the differential cross-sections at all solid angles as given by the expression

$$\sigma = \int_0^{2\pi}\int_0^{\pi}\frac{d\sigma}{d\Omega}\sin\theta d\theta d\phi\,. \quad (13)$$

The alignment parameter $A_{20}$, which is a measure of angular anisotropy of the autoionizing electrons from the *P* state, for unresolved fine structure splitting, is given as

$$A_{20} = \frac{\sigma_1 - \sigma_0}{\sigma} \quad (14)$$

In Equation 14 $\sigma_0$ and $\sigma_1$ give the total cross-sections for the magnetic sublevels 0 and 1 respectively.

## RESULTS AND DISCUSSIONS

We have calculated the differential cross sections, integral cross sections, and alignment parameters for the excitation cross sections under consideration in the energy range of near threshold energies up to 1000 eV. Figure 1*a* shows a variation of integral cross sections $\sigma(^2P)$ for electron impact excitation of the combined $^2P_{1/2}$ and $^2P_{3/2}$ states (i.e., of the unresolved $^2P$ state) of rubidium with projectile electron energy from 15.4 *eV* to 20 *eV* while Figure 1*b* shows the variation from 15.5 $eV$ to 1000 $eV$ electron impact energies. The low energy results have been separated to have a good resolution and hence a meaningful comparison of different results. The present distorted wave results with the exchange effect included are abbreviated as DWME while the present results without the exchange effect are abbreviated as DWMD. In the case where we have used the double-zeta wave functions in place of the multi-zeta wave functions we used the abbreviation DWME-DZ.

Here for the sake of clarity and to provide meaningful analyses we have mainly compared our own calculations (DWME and DWMD) obtained for the total cross sections of the lowest autoionizing state of rubidium evaluated in the present model between themselves and with the available selected experimental [6-7] and theoretical results of Borovik *et al.*, [6], theoretical results of Pangatiwar and Srivastava [13] and those of Kaur and Srivastava [12].

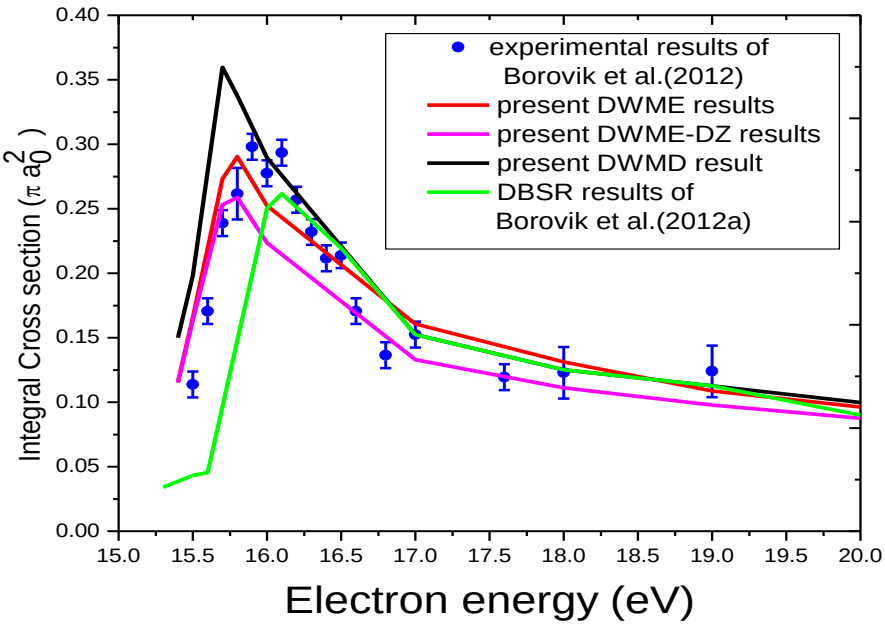


**Figure 1a.** Integral cross sections for electron impact excitation of the combined $^2P_{1/2}$ and $^2P_{3/2}$ states of rubidium as a function of projectile electron energy near threshold i. e. from 15.3 *eV* to 20 *eV*

Figure 1*a* shows that the present DWME and DWMD results for integral cross sections are in good agreement with experimental results of Borovik *et al.*, [6-7]. Precisely, the present distorted wave results are in much better agreement with the experimental results than the relativistic DBSR results of Borovik *et al*. [6]. Furthermore, the present DWMD results are higher than the DWME results at near threshold energies. It is observed that there is an abrupt increase in the integral cross sections at electron energy just above threshold energy of the lowest autoionizing state of rubidium (15.31 *eV*) and it peaks at about 15.8 *eV*. Possibly at this low energy the rubidium atom and the projectile electron form a composite state of negative ion $Rb^-$ which then decays into the rubidium atom in the autoionizing state and a free scattered electron with very low energy which explains the threshold behavior (sharp increase in the cross section near threshold energy). We can say that to a large extent, the distortion potential and exchange effects are taking account of this situation in the distorted wave method and hence giving good results as predicted by Pangantiwar and Srivastava [13].

From Figure 1*b*, it is observed that the present results are in qualitative agreement with the results of Pangatiwar and Srivastava [13] and those of Kaur and Srivastava [12] for all incident projectile energies. At low and intermediate projectile energies the present results are slightly higher than those of Pangatiwar and Srivastava [13]. This difference could be attributed to the fact that they used multi zeta Hartree Fock wave functions by Clementi *et al.*, [20] whereas we have used multi-zeta and double-zeta Hartree Fock wave functions by Clementi and Roetti [18]. It could also be as a result of the choice of the distortion potentials. Their distortion potential was the initial state static potential for the initial channel and the final state static potential for the final channel. More importantly, we have evaluated the exchange term exactly i.e., we have considered the exchange effects in the transition matrix by fully antisymmetrizing the total wave functions and also in solving the distorted electron waves. In Pangatiwar and Srivastava's calculations [13] the distorted wave was obtained by using the local exchange approximation.

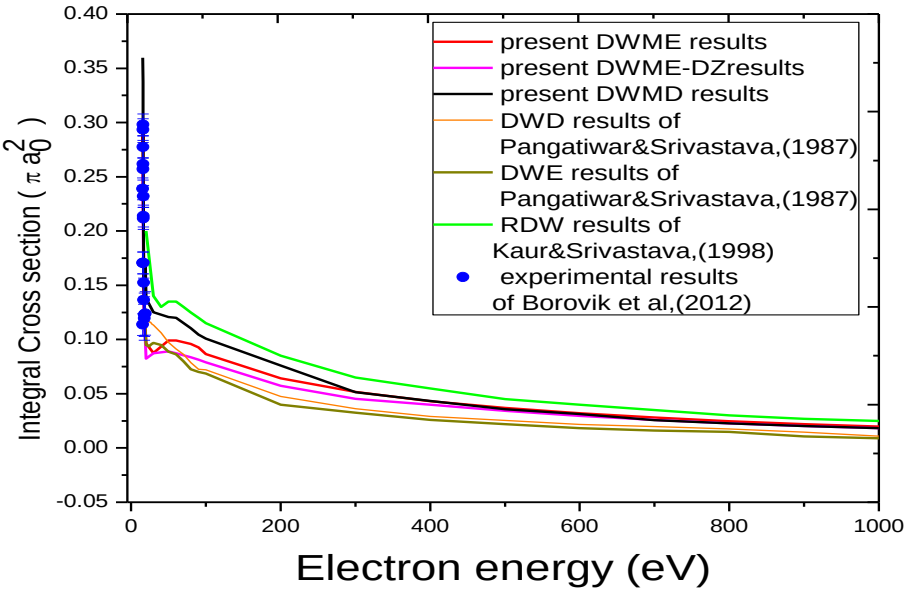


**Figure 1b**. integral cross section for electron impact excitation of $(4p^6 5s)^2 S_{1/2} - (4p^5 5s^2)^2 P$ states of rubidium as a function of projectile electron energy from near threshold to 1000 *eV*

The close agreement our results and those of Kaur and Srivastava [12] nearly at all incident energies could be associated by the fact that in the relativistic distorted wave (RDW) calculations the exchange effects are taken exactly by proper antisymmetrization of the total wave functions in the transition matrix and in solving the distorted electron waves (through Dirac equations). The difference between the present results and those of Kaur and Srivastava [12] could be as a result of the wave functions (since they used Dirac Fock wave functions in their relativistic distorted wave approximations whereas we used double zeta Hartree Fock wave functions) and the choice of the distortion potentials. Their distortion potential was sum of the static potential calculated in the final state and the exchange potential of Furness and McCarthy [21] for both channels.

The present double-zeta results are lower than multi-zeta results at all incident projectile energies. It can also be seen that the double-zeta wave functions underestimate the excitation cross sections at all energies.

Figure 2*a* shows a variation of DWME and DWMD alignment parameter for the excitation of $4p^5\ 5s^2\ ^2P$ state of rubidium with projectile electron energies from 15.31 *eV* to 100 *eV*.

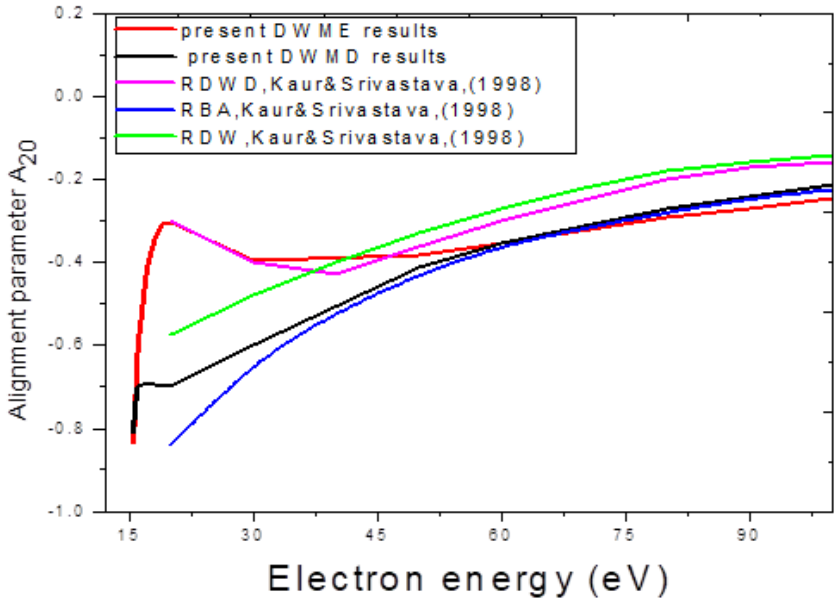


**Figure 2a**. Alignment parameter, $A_{20}$, for the excitation of for electron impact excitation of $(4p^6 5s)^2 S_{1/2} - (4p^5 5s^2)^2 P$ state of rubidium as a function of projectile electron energy from near threshold to 100 $eV$

In each case, we have compared the present results with the relativistic distorted wave results (namely RDW and RDWD) and the relativistic Born approximation (RBA) results of Kaur and Srivastava [12]. It is observed from the figures 2a and 2b the present alignment parameter results are in good qualitative agreement with RDWD of Kaur and Srivastava [12]. At projectile energies above 50 *eV* the present results are slightly lower. Below 50 *eV*, the present results are slightly higher however there is agreement in shape.

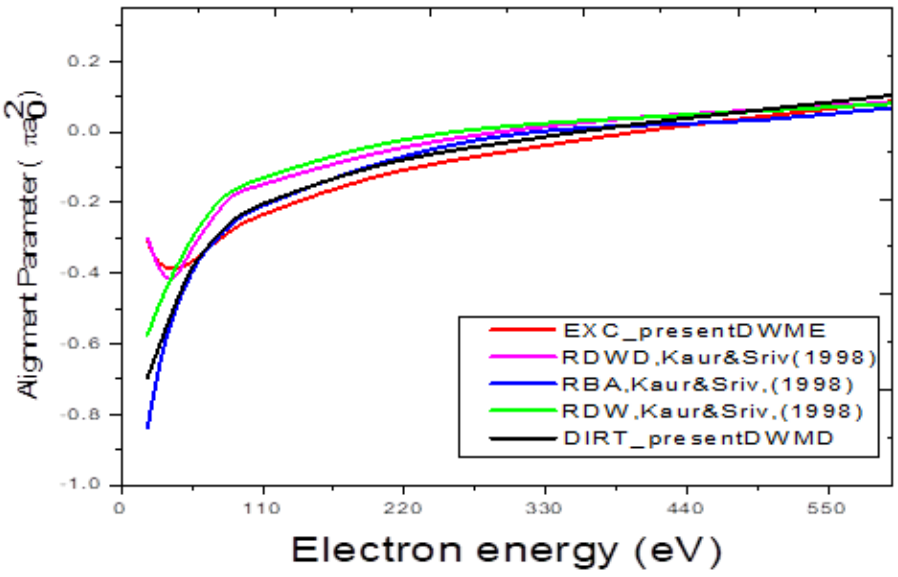


**Figure 2b**. Alignment parameter, $A_{20}$, for the excitation of for electron impact excitation of $(4p^6 5s)^2 S_{1/2} - (4p^5 5s^2)^2 P$ state of rubidium as a function of projectile electron energy from near threshold to high incident projectile energies (600 *eV*)

Moreover, the present DWME and DWMD alignment parameter results also show a maximum at about 20 *eV*. Even though there are no experimental results to confirm this maximum, it is interesting to note that in case of potassium $K^*(3p^5\ 4s^2\ ^2P)$ and sodium $Na^*(2p^5\ 3s^2\ ^2P)$, Matterstock *et al*.,[22] and DuBois *et al*., [23] respectively have obtained a similar maximum near threshold. Furthermore, we note that the difference between the target wave functions in the present model and in the calculations of Kaur and Srivastava [12] is not important for the alignment at high energies, as can be seen from the good agreement between both calculations in the energy region where plane wave Born approximation (PWBA) is valid.

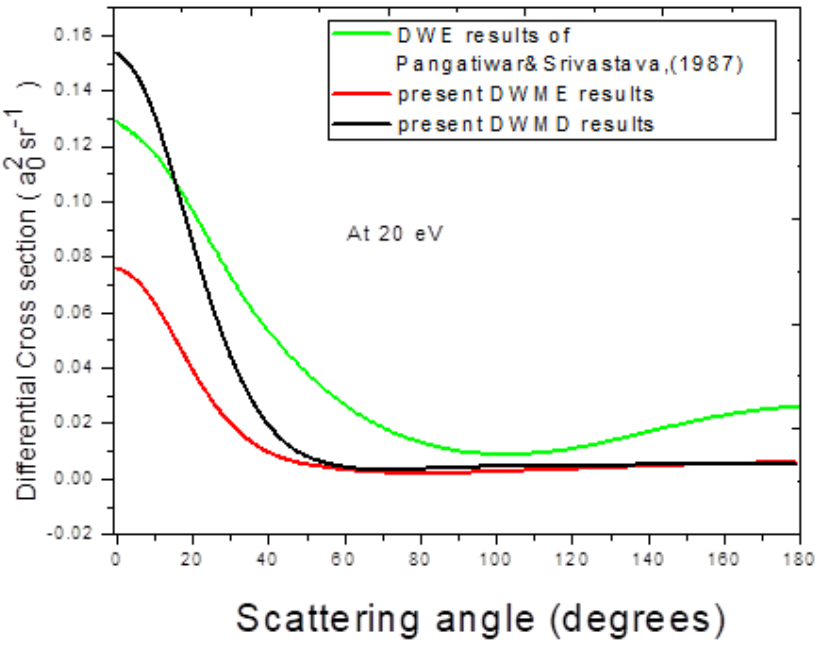


**Figure 3a.** Differential cross sections for the excitation of for electron impact excitation of $(4p^6 5s)^2 S_{1/2} - (4p^5 5s^2)^2 P$ state of rubidium as a function of scattering angles at an incident projectile energy of 20 *eV*.

Figures 3*a*, 3*b*,3*c*, 3*d* and 3*e* show variation of DWME and DWMD differential cross sections with scattering angles, at projectile energies 20 *eV*, 30 *eV*, 50 *eV*, 100 *eV* and 200 *eV*, respectively. The only results available to us for comparison are those of Pangatiwar and Srivastava [13].

Figure 3*a* shows that at 20 $eV$ the present results (DWME and DWMD) are in qualitative agreement with the results of Pangatiwar and Srivastava [13] at all scattering angles.

The results of Pangatiwar and Srivastava [12] are slightly higher than the present results at nearly all scattering angles. Fig 3*b* shows that at 30 $eV$ both results (present and Pangatiwar and Srivastava's [13]) are in excellent agreement at higher scattering angles (> 60 degrees) but at lower angles the agreement is not that good. Figure 3*c* shows that at 50 *eV* both results behave the same way as in the case of Figure 3b (at 30 *eV*) i.e., the agreement is excellent for higher scattering angles (>40 degrees) but at lower scattering angles it is not so good. From Figure 3*d* it is observed that at 100 *eV* the behavior is the same except that the Pangatiwar and Srivastava's [13] results give higher values at scattering angles greater than 120 degrees. Figure 3*e* shows that when the incident energy increases to 200 *eV* the present DWME and DWMD results almost coincide nearly at all scattering angles. This means that effect of exchange is ignorable at high projectile energies hence excitation here is mainly through direct process.

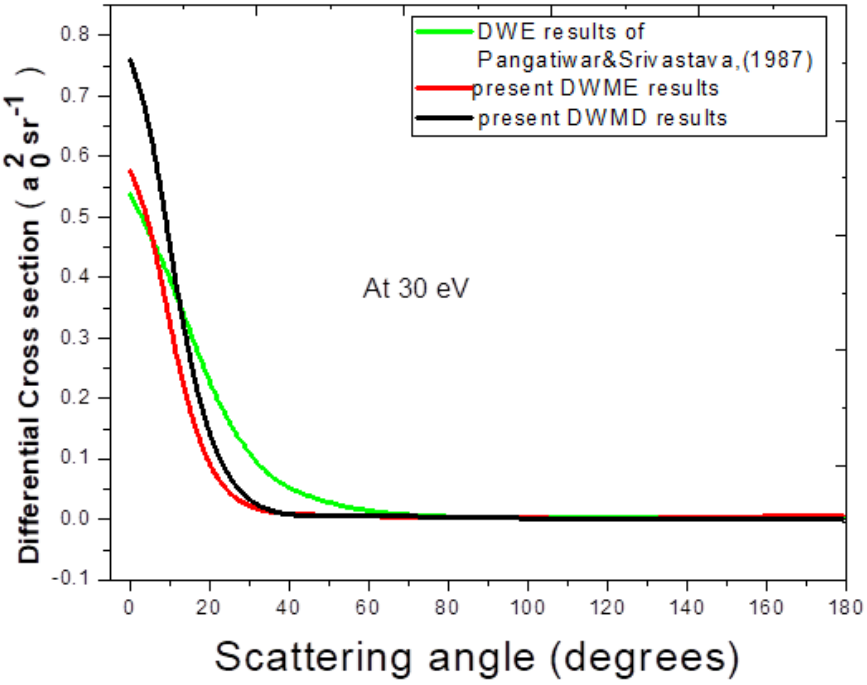


**Figure 3b**. Differential cross sections for the excitation of for electron impact excitation of $(4p^6 5s)^2 S_{1/2} - (4p^5 5s^2)^2 P$ state of rubidium as a function of scattering angles at an incident projectile energy of 30 *eV*.

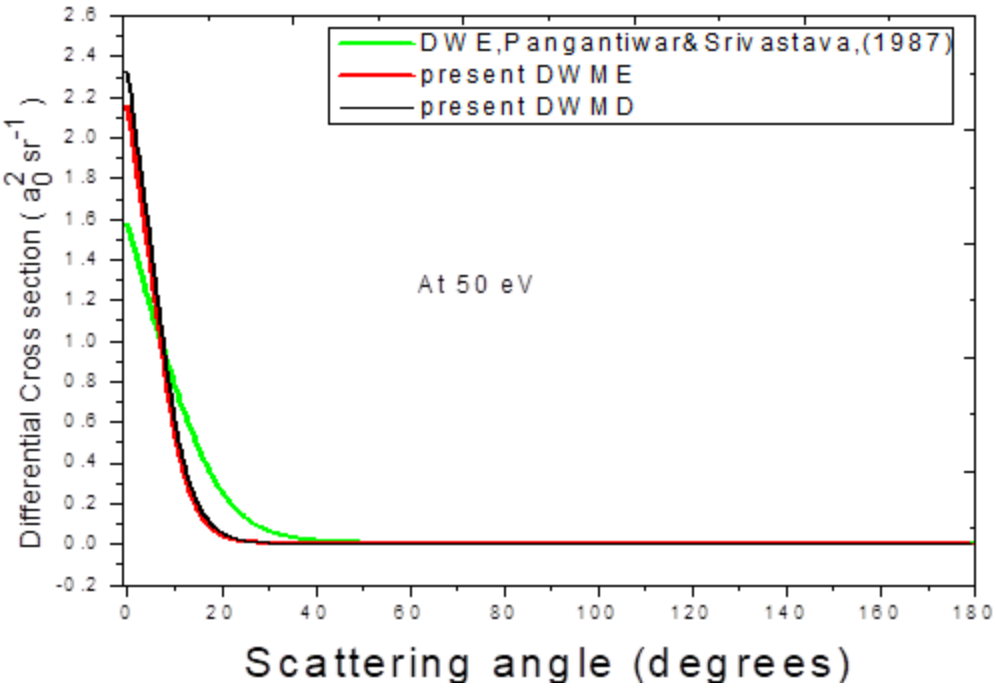


**Figure 3c.** Differential cross sections for the excitation of for electron impact excitation of $(4p^6 5s)^2 S_{1/2} - (4p^5 5s^2)^2 P$ state of rubidium as a function of scattering angles at an incident projectile energy of 50 *eV*.

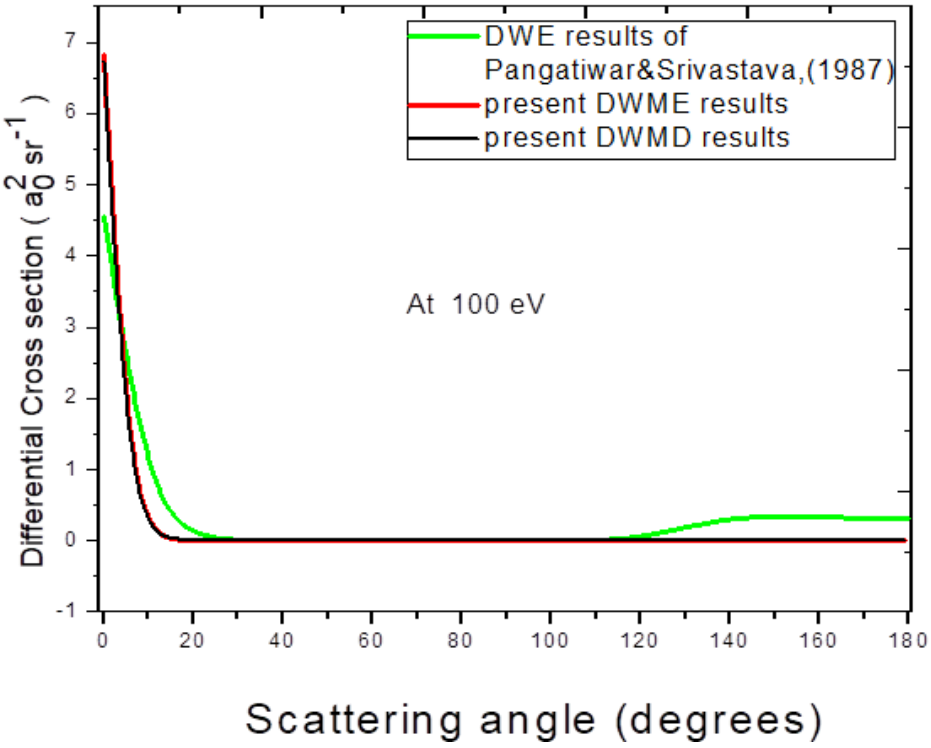


**Figure 3d**. Differential cross sections for the excitation of for electron impact excitation of $(4p^6 5s)^2 S_{1/2} - (4p^5 5s^2)^2 P$ state of rubidium as a function of scattering angles at an incident projectile energy of 100 *eV*.

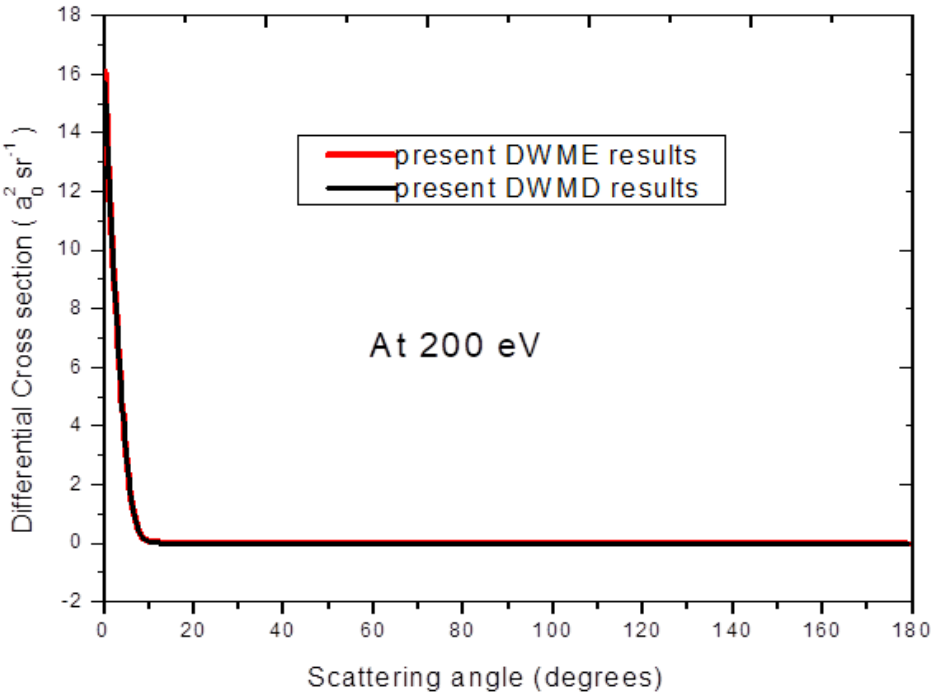


**Figure 3e**. Differential cross sections for the excitation of for electron impact excitation of $(4p^6 5s)^2 S_{1/2} - (4p^5 5s^2)^2 P$ state of rubidium as a function of scattering angles at an incident projectile energy of 200 *eV*.

## CONCLUSION

The present work reports the results of electron impact excitation of the lowest autoionizing state of rubidium using distorted wave method with a variation in the distortion potential. Using this method, we evaluated the integral cross section, differential cross sections, and alignment parameter for *4p - 5s* excitation considering both direct and exchange contribution. The results show that the method employed in this study is successful in predicting the near threshold resonant structure observed in the experimental integral cross section results of Borovik *et al.*, [6-7]. This structure can be attributed to exchange process between the projectile electron and one of the core target electrons, and the formation of negative rubidium ion at near threshold energies. It is very surprising that the present distorted wave results compare very well with the experimental results than does the DBSR results of Borovik *et al.*, [6]. Checking these results further with inclusion of polarization, exchange and absorption potentials in the distortion potential used for the projectile electron would be interesting.

## ACKNOWLEDGEMENT

The author expresses gratitude to Prof. C. S. Singh of Kenyatta University, Republic of Kenya, whose extensive experience in the field of atomic collisions was exceedingly beneficial in the success of this work.

## REFERENCES

1 Joachain, C. J. 1975. Quantum collision theory.
2 Ross, K. J. & Ottely, T. W. 1975. Ejected electron spectrum of rubidium autoionizing levels obtained by electron impact excitation, *Phys. Lett. A*, 54, 57-58.
3 Nygaard, K. J. 1975. Electron impact autoionization in heavy alkali metals. *Physical review A*, *11*(4), 1475.
4 Stapelfeldt, H., Kristensen, P., Ljungblad, U., Andersen, T., & Haugen, H. K. 1994. Autoionizing states of negative ions in strong resonant laser fields: The negative rubidium ion. *Physical Review A*, *50*(2), 1618.
5 Borovik, A. A. 2011. Radiative transitions in the system of autoionizing levels of cesium atoms excited by electron impact. *Optics and Spectroscopy*, *110*, 680-685.
6 Borovik, A., Ilyashevytch, V., Zatsarinny, O., & Bartschat, K. 2012, Nov Resonance excitation of the ($4p^5 5s^2$) $^2P_{3/2,\,1/2}$ autoionizing states in Rb atoms by electron impact. In *Journal of Physics: Conference Series* (Vol. 388, No. 4, p. 042009). IOP Publishing.
7 Borovik, A., Roman, V., & Kupliauskienė, A. 2012. The $4p^6$ autoionization cross section of Rb atoms excited by low-energy electron impact. *Journal of Physics B: Atomic, Molecular and Optical Physics*, *45*(4), 045204.
8 Srivastava, R., & Rai, D. K. 1977. Excitation of autoionizing levels in the collision of electrons with alkali-metal atoms. *Journal of Physics B: Atomic and Molecular Physics*, *10*(2), 269.
9 Srivastava, R., Singh, C. S., & Rai, D. K. 1982. Excitation of the lowest autoionising states in alkalis. *Journal of Physics B: Atomic and Molecular Physics*, *15*(12), 1899.
10 Singh, C. S. 2004. Magnetic-sublevel differential cross sections for electron-impact excitation of 21P state of helium. *East African Journal of physical sciences*, *5*, 85-98.
11 Tiwary, S. N., & Rai, D. K. 1975. Electron impact excitation of the lowest autoionizing level in alkali metal atoms. *Journal of Physics B: Atomic and Molecular Physics*, *8*(7), 1109.
12 Kaur, S., & Srivastava, R. 1999. Excitationof the lowest autoionizing $np^5(n+1)\,s^2$, $^2P_{3/2,\,1/2}$ states of Na (n= 2), K (n= 3), Rb (n= 4) and Cs (n= 5) byelectron impact. *Journal of Physics B: Atomic, Molecular and Optical Physics*, *32*(10), 2323.
13 Pangantiwar, A. W., & Srivastave, R. 1987. e+ or-impact excitation of autoionising levels in alkalis: a distorted-wave approach. *Journal of Physics B: Atomic and Molecular Physics*, *20*(21), 5881.

14 Pangantiwar, A. W., & Srivastava, R. 1988. Excitation of the rubidium atom by electrons and positrons: differential cross section and correlation parameters. *Journal of Physics B: Atomic, Molecular and Optical Physics*, *21*(23), 4007.
15 McDaniel, E. W. 1989. Atomic collisions: electron and photon projectiles.
16 Crothers, D., & McCarroll, R. 1965. Excitation of neutral atoms by electron impact. *Proceedings of the Physical Society*, *86*(4), 753.
17 Roy, B. N., & Rai, D. K. 1973. Electron-impact ionization of Alkali metals. *Physical Review A*, *8*(2), 849.
18 Clementi, E., & Roetti, C. 1974. Roothaan-Hartree-Fock atomic wavefunctions: Basis functions and their coefficients for ground and certain excited states of neutral and ionized atoms, $Z \leq 54$. *Atomic data and nuclear data tables*, *14*(3-4), 177-478.
19 Madison, D. H., & Bartschat, K. 1996. The distorted-wave method for elastic scattering and atomic excitation. In *Computational atomic physics: Electron and positron collisions with atoms and ions* (pp. 65-86). Berlin, Heidelberg: Springer Berlin Heidelberg.
20 Clementi, E., Raimondi, D. L., & Reinhardt, W. P. 1967. Atomic screening constants from SCF functions. II. Atoms with 37 to 86 electrons. *Journal of Chemical Physics*, *47*(4), 1300-1307.
21 Furness, J. B., & McCarthy, I. E. 1973. Semiphenomenological optical model for electron scattering on atoms. *Journal of Physics B: Atomic and Molecular Physics*, *6*(11), 2280.
22 Matterstock, B., Huster, R., Paripast, B., & Grum-Grzhimailoz, N. Excitation of K*($3p^5$ $4s^2$ $^2P_{3p}$, $^2P_{1/2}$) by electron impact in the range from near threshold to 500 eV: alignment and cross section ratios. *Journal Physic B: Atomic Molecular Optic Physic*, 28, 4301-4309.
23 DuBois, R. D., Mortensen, L., & Rodbro, M. 1981. Collisionally induced alignment produced by electron and light-ion impact: Auger electron emission following 2p ionisation and excitation. *Journal of Physics B: Atomic and Molecular Physics*, *14*(10), 1613.
24 Andersen, N. & Bartschat, K. 1993. *Comment*. *At. Mol. Phys*. 29, 157-88
25 Bray, I. 1995. Calculation of electron-impact ionization of lithium-like targets. *Journal of Physics B: Atomic, Molecular and Optical Physics*, *28*(7), L247.
26 Jobunga, E., Okumu, J., & Singh, C. S. 2012. Excitation cross-section evaluation for the lowest auto-ionizing state of potassium. *The African Review of Physics*, *7*.